Pure Appl. Chem., Vol. 71, No. 9, pp. 1727–1740, 1999.
Printed in Great Britain.

Metal ion-binding properties of the antiviral nucleotide analogue 9-[2-(phosphonomethoxy)ethyl]adenine (PMEA). Why is its diphosphorylated form, $PMEApp^{4-}$, initially a better substrate for nucleic acid polymerases than (2′-deoxy)-adenosine 5′-triphosphate ($dATP^{4-}$/ATP^{4-})?*

Helmut Sigel

Institute of Inorganic Chemistry, University of Basel, Spitalstrasse 51, CH-4056 Basel, Switzerland

Abstract: The metal ion-coordinating properties (Mg^{2+}, Mn^{2+}, Zn^{2+}, etc. = M^{2+}) are summarized for (i) the dianion of 9-[2-(phosphonomethoxy)ethyl]adenine ($PMEA^{2-}$ = adenine (9)-CH_2CH_2-O-CH_2-PO_3^{2-}) and (ii) methylphosphonylphosphate ($MePP^{3-}$ = $CH_3P(O)_2^-$-O-PO_3^{2-}). The observed increased stability of the M(PMEA) complexes is mostly due to the formation of five-membered chelates involving the ether oxygen of the -CH_2-O-CH_2-PO_3^{2-}residue; with some metal ions (Ni^{2+}, Cu^{2+}) in addition an interaction with N3 of the adenine residue occurs. The $M(MePP)^-$ complexes are also somewhat more stable than those of diphosphate monoesters, like methyl diphosphate, because of the enhanced basicity of the phosphonyl unit. These two observations provide an explanation for the fact that diphosphorylated $PMEA^{2-}$, an analogue of (d)ATP^{4-}, is initially a better substrate for several nucleic acid polymerases than $dATP^{4-}$. The higher basicity of the phosphonyl group and the formation of the five-membered chelates favor $PMEApp^{4-}$ over $dATP^{4-}$ because they facilitate the M(α)-M(β,γ) coordination pattern needed for the enzyme-catalyzed incorporation of the substrate in the growing nucleic acid chain.

SOME BACKGROUND INFORMATION

Viral infections are among the most common causes of illnesses such as influenza, pox, polio, and herpes. After entering cells, viruses use the genetic machinery of the host for their own replication. The advent of the human immunodeficiency virus (HIV) has spurred intense research toward the mechanisms of viral infection and replication with the aim to develop antiviral drugs. Indeed, viral replication can be interrupted in various ways [1]. For example, since the genetic information is stored in nucleic acids (DNA and RNA), their catalytic synthesis by polymerases could be blocked and thus (reverse) transcription be inhibited. Considering further that nucleoside 5′-triphosphates (in particular ATP^{4-}), which are at the center of many metabolic processes [2,3], are the substrates for nucleic acid polymerases, it is not surprising that nucleoside derivatives, phosphorylated or not, are intensely investigated for their antiviral action [4,5].

Nucleoside analogues, like acyclovir, need to be transformed into active metabolites [5] by the consecutive action of nucleoside and nucleotide kinases. To avoid the first phosphorylation step,

* Invited lecture presented at the 26th International Conference on Solution Chemistry, Fukuoka, Japan, 26–31 July 1999, pp. 1691–1764.
Correspondence: E-mail: Helmut.Sigel@unibas.ch

nucleotide analogues were developed which contain the phosphonomethyl ether group as an isopolar and nondegradable equivalent [4,5] of the α-phosphoryl group [6]. One of the most promising antivirals of this class is 9-[2-(phosphonomethoxy)ethyl]adenine (PMEA) [5,7]; it can be considered as an acyclic-nucleoside phosphonate analogue of (2′-deoxy)-adenosine 5′-monophosphate ((d)AMP^{2-}) and indeed, it mimics well the properties of its parent nucleotide from a structural point of view [8] as well as in its reactions [9,10]. PMEA is shown in Fig. 1 in its anionic form, together with related nucleotides and analogues [11–14].

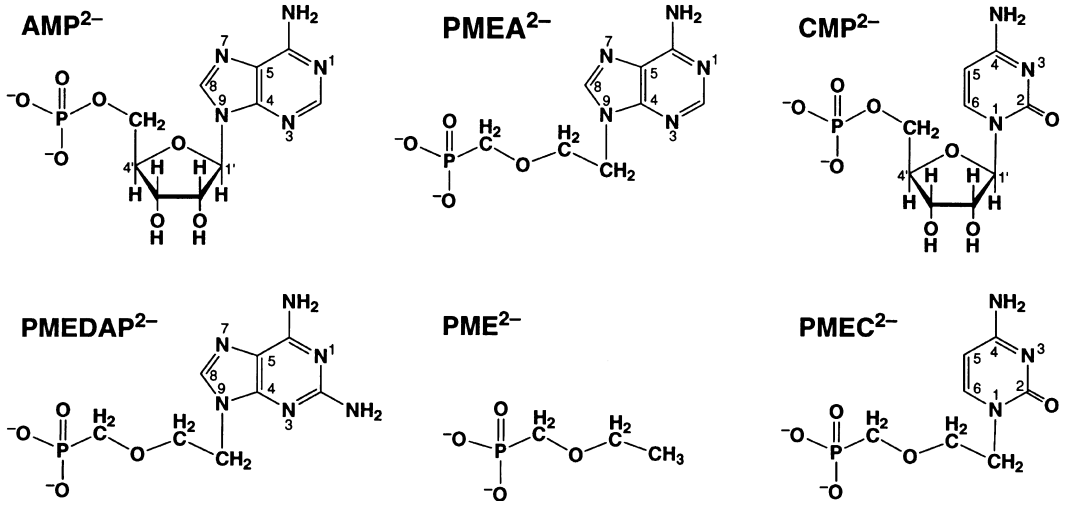

Fig. 1 Chemical structures of the dianions of 9-[2-(phosphonomethoxy)ethyl]adenine (PMEA^{2-}) [8] and 1-[2-(phosphonomethoxy)ethyl]cytosine (PMEC^{2-}) and of their parent nucleotides adenosine 5′-monophosphate (AMP^{2-}) [11–13] and cytidine 5′-monophosphate (CMP^{2-}) [13,14], respectively, which are shown in their dominating *anti* conformation. In addition the structures of the dianions of (phosphonomethoxy)ethane (PME^{2-} = ethoxymethanephosphonate) and 9-[2-(phosphonomethoxy)ethyl]-2,6-diaminopurine (PMEDAP^{2-} = dianion of 9-[2-(phosphonomethoxy)ethyl]-2-aminoadenine) are given.

PMEA is active against a variety of DNA viruses and retroviruses [4,15,16], including HIV [1,7], after its diphosphorylation by kinases [16,17] to the dATP^{4-} analogue PMEApp^{4-}. It is recognized as substrate by (viral) DNA polymerases or retroviral reverse transcriptases and incorporated in the growing nucleic acid chain, which is then terminated due to the lack of a 3′-hydroxy group [16–18], which is present in dATP^{4-}. Some results of *in vitro* experiments with PMEApp and related analogues are summarized in Table 1 [6,19]. Since PMEA and related compounds are not sufficiently bioavailable due to poor absorption, they have been formulated as diesters into an oral prodrug form; the corresponding PMEA derivative offers great promises and is now in advanced clinical trials in HIV-infected individuals [1,7].

METAL IONS AND NUCLEIC ACID POLYMERASES

Most of the relevant enzymes involved in the processes indicated above, like DNA and RNA polymerases, kinases, and ATP synthases, depend on metal ions (often Zn^{2+}) [2,3] and use nucleotides as substrates only in the form of metal ion (mostly Mg^{2+}) complexes [20]. From the *in vitro* experiments summarized in Table 1 it is evident that the larger the ratio K_m/K_i, the more pronounced is the inhibition of the DNA polymerase by the ANPpp considered. Clearly, PMEApp is an excellent inhibitor of DNA synthesis though not necessarily the best one (see also the section on Conclusions and Mechanistic Considerations). It is initially also an excellent substrate for AMV reverse transcriptase, even in the presence of a 20-fold excess of dATP. Under these conditions catalysis of the growing DNA chain is depressed to 50% after 5 min [6,19]. Could the metal ion-binding properties of PMEApp^{4-} be of relevance here, as we have suggested recently [21]?

Kinetic studies of the M^{2+}-promoted dephosphorylation of ATP^{4-} and other triphosphates [22–24] revealed that in the most reactive species one metal ion is coordinated to the α,β-phosphate groups and

Table 1 DNA polymerase and reverse transcriptase inhibition by some diphosphorylated acyclic-nucleoside phosphonate analogues (ANPpp) of nucleoside 5′-triphosphates*

Inhibitor ANPpp	Competitive substrate	HSV-1 DNA pol†,‡		HeLa cell DNA pol α‡	
		K_i (μM)	K_m/K_i	K_i (μM)	K_m/K_i
PMEApp	dATP	0.11	6.95	0.87	2.36
PMEGpp	dGTP	0.09	7.78	1.15	0.77
PMECpp	dCTP	1.27	1.41	3.04	0.49
PMEDAPpp	dATP	0.03	25.1	0.18	11.5

	Competitive substrate (20 μM)	IC_{50} (μM) of AMV rev trans§	
		3 min	5 min
PMEApp	dATP	1.35	1.00
PMEGpp	dGTP	2.50	2.10
PMECpp	dCTP	3.10	2.30
PMEDAPpp	dATP	0.23	0.18

* Compiled from tables 7 and 9 of [6] and tables 3 and 5 of [19].
† HSV = herpes simplex virus.
‡ The (apparent) kinetic constants (K_i, K_m) were probably determined by Lineweaver–Burk and/or Dixon plots as commonly done by Holý *et al*. (see, e.g. [18]).
§ Inhibitor concentration causing a 50% depression of the growing DNA chain as catalyzed by the avian myeloblastosis virus (= AMV/MAV) reverse transcriptase.

one to the terminal γ-phosphate group. This transphosphorylation mechanism was recently confirmed by an X-ray structural study [25] of *Escherichia coli* phosphoenolpyruvate carboxykinase, but already 15 years ago it was also concluded that the two activating metal ions 'may interact not only in a M(α,β)-M(γ)-like way but that a M(α)-M(β,γ) coordination can also be enforced (by an enzyme) and this would then lead to a reactive species ready for the transfer of ... a nucleoside monophosphate' unit [22]. A simplified structure of such a M_2(NTP) complex is shown in Fig. 2. Indeed, X-ray structural studies of nucleic acid polymerases confirmed the involvement of two metal ions and mechanisms similar to our earlier one [22,23] were proposed [26,27].

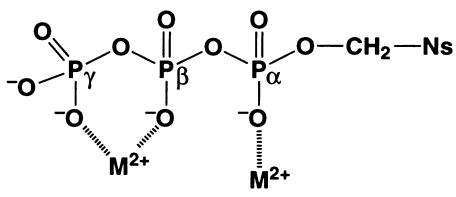

Fig. 2 Simplified structure of the M_2(NTP) complex with a M(α)-M(β,γ) coordination mode (Ns = nucleosidyl residue).

The crucial step in the polymerase mechanism indicated above is to force a metal ion into the α position of the triphosphate chain [22,23] of an NTP^{4-} (Fig. 2). Hence, one might suspect that $PMEApp^{4-}$, being initially an excellent substrate (Table 1), has in this respect an advantage over $dATP^{4-}$. Since the stabilities of M_2(PMEApp) and M_2(ATP) or M_2(dATP) complexes cannot easily be measured and compared, especially if M(α,β)-M(γ) and M(α)-M(β,γ) binding modes need to be distinguished, we decided [21] to evaluate the metal ion-binding properties of the P_α group of $PMEApp^{4-}$ by studying the crucial segments of this nucleotide analogue, i.e. $PMEA^{2-}$ and methylphosphonylphosphate.

(*i*) The complexing properties of $PMEA^{2-}$ should reveal if and to which extent the ether oxygen of the $-CH_2-O-CH_2-PO_3^{2-}$ chain (see Fig. 1) participates in M^{2+} binding, giving rise to the intramolecular Equilibrium 1 and facilitating, via the formation of the five-membered chelate, P_α-group coordination in M_2(PMEApp).

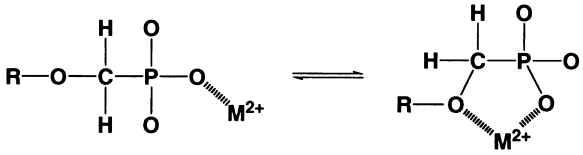

(1)

(*ii*) Since methylphosphonate is somewhat more basic than methyl phosphate as follows from the release of the primary proton from the twofold protonated species which occurs with $pK^{H}_{CH_3P(O)(OH)_2} = 2.10 \pm 0.03$ [28] and $pK^{H}_{CH_3OP(O)(OH)_2} = 1.1 \pm 0.2$ [29], respectively, the M^{2+}-binding properties of $MePP^{3-}$ are expected to be somewhat more pronounced than those of methyl diphosphate or any other simple diphosphate monoester (Fig. 3).

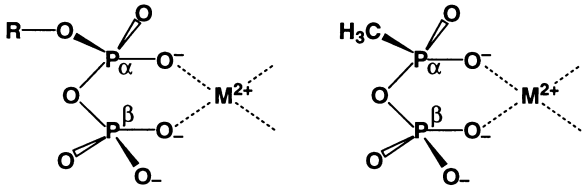

Fig. 3 Formal structures of the M^{2+} complexes of a diphosphate monoester (R-DP^{3-}; R = noncoordinating residue) (left) and methylphosphonylphosphate ($MePP^{3-}$) (right). [The IUPAC name of the Na_3(MePP) salt is phosphoric methylphosphonic monoanhydride trisodium salt.]

Indeed, as will be summarized below, both points are in favor of metal ion binding at the P_α group, facilitating the M(α)-M(β,γ)-binding mode in M_2(PMEApp).

EVALUATION OF THE METAL ION-BINDING PROPERTIES OF PMEA

General aspects and definition of equilibrium constants

$PMEA^{2-}$ can accept four protons [8], but only the first two bound are relevant for the physiological pH range [30]. Hence, Eqns 2 and 3 need to be considered (NP^{2-} = nucleobase phosph(on)ate derivative):

$$H_2(NP)^{\pm} \rightleftharpoons H^+ + H(NP)^- \tag{2a}$$

$$K^{H}_{H_2(NP)} = [H^+][H(NP)^-]/[H_2(NP)^{\pm}] \tag{2b}$$

$$H(NP)^- \rightleftharpoons H^+ + NP^{2-} \tag{3a}$$

$$K^{H}_{H(NP)} = [H^+][NP^{2-}]/[H(NP)^-] \tag{3b}$$

Comparison of relevant results assembled in Table 2 [12,30–38] reveals that the first of the two protons is always released from the nucleobase and the second one from the monoprotonated phosph(on)ate residue. Hence, if the stability of metal ion complexes is determined by potentiometric pH titration, Eqns 4 and 5 need to be considered:

$$M^{2+} + H(NP)^- \rightleftharpoons M(H;NP)^+ \tag{4a}$$

$$K^{M}_{M(H;NP)} = M(H;NP)^+]/([M^{2+}][H(NP)^-]) \tag{4b}$$

$$M^{2+} + NP^{2-} \rightleftharpoons M(NP) \tag{5a}$$

$$K^{M}_{M(NP)} = M(NP)]/([M^{2+}][NP^{2-}]) \tag{5b}$$

Table 2 Comparison of the acid–base properties of some acyclic-nucleoside phosphonates with their parent nucleoside 5′-monophosphates and some related constituents, as determined by potentiometric pH titrations* (aqueous solution; 25 °C; $I = 0.1$ M, $NaNO_3$)†

Protonated species	pK_a for the sites:		Ref.
	$(N1)H^+$ (cf.‡)	$P(O)_2(OH)^-$	
$H(adenosine)^+$	3.61 ± 0.03		12
$H(RibMP)^-$		6.24 ± 0.01	31
$H_2(AMP)^{\pm}$	3.84 ± 0.02	6.21 ± 0.01	32,33
$H(9\text{-methyladenine})^+$	4.10 ± 0.01		34
$H(PME)^-$		7.02 ± 0.01	30
$H_2(PMEA)^{\pm}$	4.16 ± 0.02	6.90 ± 0.01	30
$H_2(PMEDAP)^{\pm}$	4.82 ± 0.01	6.94 ± 0.01	35
$H(cytidine)^+$	4.14 ± 0.02		36
$H_2(CMP)^{\pm}$	4.33 ± 0.04	6.19 ± 0.02	31
$H_2(dCMP)^{\pm}$	4.46 ± 0.01	6.24 ± 0.01	37
$H_2(PMEC)^{\pm}$	4.72 ± 0.01	6.95 ± 0.01	38

* So-called practical, mixed or Brønsted constants are listed [39].
† The errors given are three times the standard error of the mean value or the sum of the probable systematic errors, whichever is larger.
‡ In the cytosines (last four entries) H^+ is located at N3 (see Fig. 1).

Values for Eqn 4 have been determined [30]; usually, the stability of these protonated complexes is rather low and their formation degree is not of relevance for the physiological pH range; consequently, they are not considered further here. The stability constants for the M(PMEA) complexes according to Eqn 5 are listed in column 2 of Table 3 [30,33,35,38,40,41].

Formation of two isomeric M(PMEA) complexes. Participation of the ether oxygen in metal ion binding

A few examples of log $K^{M}_{M(PMEA)}$ values (Eqn 5) are plotted in dependence on p$K^{H}_{H(PMEA)}$ (●) (Eqn 3) in Figure 4 together with the straight line plots log $K^{M}_{M(R\text{-}PO_3)}$ vs. p$K^{H}_{H(R\text{-}PO_3)}$ [30] for simple phosph(on)ate ligands like phenyl phosphate [31] or methylphosphonate [30] and the corresponding data [30] for the M(PME)/$H(PME)^+$ systems (⊗). These data pairs as well as those for M(PMEA)/$H(PMEA)^+$ are above their reference lines demonstrating an increased complex stability. Hence, a further interaction aside from the one with the phosphonate group must take place [42]; due to the results with PME (Fig. 4) this can only be the ether oxygen of the $\text{-}CH_2\text{-}O\text{-}CH_2\text{-}PO_3^{2-}$ residue (Fig. 1). Hence, Equilibrium 1 operates.

Obviously, the vertical distance between a data point (●/⊗) in Fig. 4 and its reference line reflects [42] the stability of the five-membered chelate. Based on the straight-line equations (listed in [30]) and the p$K^{H}_{H(NP)}$ values, the stability constant for $\text{-}PO_3^{2-}/M^{2+}$ binding can be calculated (calc.) for any M(NP) complex for which the pK_a value of $H(NP)^-$ is known. The vertical distances in Fig. 4 are thus defined by Eqn 6, where $K^{M}_{M(NP)}$ represents the experimentally measured stability constant. The results according to Eqn 6 are listed in column 4 of Table 3 for the M(PMEA) complexes; they are positive for all 10 metal ions studied confirming that Equilibrium 1 operates.

$$\log \Delta = \log \Delta_{M/NP} = \log K^{M}_{M(NP)} - \log K^{M}_{M(NP)_{calc.}} \quad (6)$$

$$\Delta \log \Delta = \log \Delta_{M/PMEA} - \log \Delta_{M/PME\text{-}R} \quad (7)$$

For comparison, the results of related systems are listed in columns 5 and 6. From the difference defined in Eqn 7, where log $\Delta_{M/PME\text{-}R}$ refers to a PME derivative with a noncoordinating nucleobase

Table 3 Stability constant comparisons for the M(PMEA) complexes between the measured (exptl [30]) (Eqn 5) and the calculated stability constants (calc.) based on the basicity of the phosphonate group in $PMEA^{2-}$ ($pK^{H}_{H(PMEA)} = 6.90$; Table 2) and the baseline equations established previously [30] (see also Fig. 4 and [33,40,41]), together with the resulting evidence for an increased complex stability, log $\Delta_{M/PMEA}$, as defined by Eqn 6. The stability enhancements for M(PME) (log $\Delta_{M/PME}$ [30]) and M(PME-R) complexes (log $\Delta_{M/PME\text{-}R}$ [38]), where R represents a non-coordinating nucleobase residue, are given for comparison. The values for $\Delta\log\Delta$ according to Eqn 7 result from the comparison between the stability enhancements for the M(PMEA) and M(PME-R) complexes (aqueous solution; 25 °C; $I = 0.1$ M, $NaNO_3$)*

	$\log K^{M}_{M(PMEA)}$					
M^{2+}	exptl	calc.	$\log \Delta_{M/PMEA}$	$\log \Delta_{M/PME}$	$\log \Delta_{M/PME-R}$	$\Delta \log \Delta$
Mg^{2+}	1.87 ± 0.04	1.71 ± 0.03	0.16 ± 0.05	0.22 ± 0.03	0.16 ± 0.04	0.00 ± 0.06
Ca^{2+}	1.65 ± 0.05	1.54 ± 0.05	0.11 ± 0.07	0.14 ± 0.05	0.12 ± 0.05	−0.01 ± 0.09
Sr^{2+}	1.37 ± 0.03	1.30 ± 0.04	0.07 ± 0.05	0.07 ± 0.05	0.09 ± 0.05	−0.02 ± 0.07
Ba^{2+}	1.30 ± 0.05	1.22 ± 0.04	0.08 ± 0.06	0.10 ± 0.05	0.11 ± 0.05	−0.03 ± 0.08
Mn^{2+}	2.54 ± 0.06	2.33 ± 0.05	0.21 ± 0.08	0.27 ± 0.05	0.19 ± 0.06	0.02 ± 0.10
Co^{2+}	2.37 ± 0.03	2.09 ± 0.06	0.28 ± 0.07	0.29 ± 0.06	0.20 ± 0.06	0.08 ± 0.09
Ni^{2+}	2.41 ± 0.05	2.11 ± 0.05	0.30 ± 0.07	0.19 ± 0.05	0.14 ± 0.07	0.16 ± 0.10
Cu^{2+}	3.96 ± 0.04	3.19 ± 0.06	0.77 ± 0.07	0.48 ± 0.07	0.48 ± 0.07	0.29 ± 0.10
Zn^{2+}	(2.66 ± 0.13)†	2.36 ± 0.06	0.30 ± 0.10	0.34 ± 0.06	0.29 ± 0.07	0.01 ± 0.12
Cd^{2+}	3.00 ± 0.04	2.67 ± 0.05	0.33 ± 0.06	0.30 ± 0.05	0.30 ± 0.05	0.03 ± 0.08

* Regarding the error limits (3σ) see footnote † of Table 2. The error limits (3σ) of the derived data, in the present case, e.g. for column 4, were calculated according to the error propagation after Gauss.

† No stability constant could be determined owing to precipitation. The above value is an estimate; see table 7 of [30]. An estimate for the stability constant of the monoprotonated $Zn(H;PMEA)^{+}$ complex is found in table 3 of [35]: $\log K^{Zn}_{Zn(H;PMEA)} = 1.15 \pm 0.3$.

residue, follows that for all M(PMEA) complexes, except those with Ni^{2+}, Cu^{2+}, and possibly also Co^{2+}, the observed stability increase can solely be explained by the ether oxygen–metal ion interaction.

The position of Equilibrium 1 is defined by the intramolecular and dimensionless constant, $K_{I/O}$, which can be calculated with Eqn 8 (for details see [30,33,40]), where $M(NP)_{op}$ is the open isomer and $M(NP)_{cl/O}$ the closed or chelated one:

$$K_{I/O} = [M(NP)_{cl/O}]/[M(NP)_{op}] = 10^{\log \Delta} - 1 \quad (8)$$

The percentage of the closed species follows from Eqn 9:

$$\%\ M(NP)_{cl/O} = 100 \cdot K_{I/O}/(1 + K_{I/O}) \quad (9)$$

The results based on Eqns 8 and 9 are given in Table 4 for all those M(PMEA) complexes for which $\Delta\log\Delta = 0$ within the error limits (see the final column in Table 3). For example, for the biologically relevant metal ions Mg^{2+} and Zn^{2+}, the formation degree of $M(PMEA)_{cl/O}$ amounts to about 30 and 50%, respectively, proving that Equilibrium 1 is of importance.

Formation of a third isomer involving the adenine residue of $PMEA^{2-}$

For Ni^{2+} and Cu^{2+}, and most probably also Co^{2+}, the stability enhancement, log $\Delta_{M/PMEA}$ (Eqn 6), cannot solely be explained by the ether oxygen interaction, since the values for the difference between the differences, i.e. $\Delta\log\Delta$ (Eqn 7), are positive and hence, the nucleobase residue of $PMEA^{2-}$ must also be involved in metal ion binding. The only sites which are sterically accessible are N3 and N7 [30,40,43].

N3 can only participate in metal ion binding if the ether oxygen remains in the coordination sphere of the metal ion, i.e. when not only the five-membered ring of Equilibrium 1 but in addition also a seven-membered one with N3 is formed; this species is designated as $M(NP)_{cl/O/N3}$. The participation of N7 can only occur via macrochelate formation of an already -PO_3^{2-}-bound M^{2+}; this species is designated as

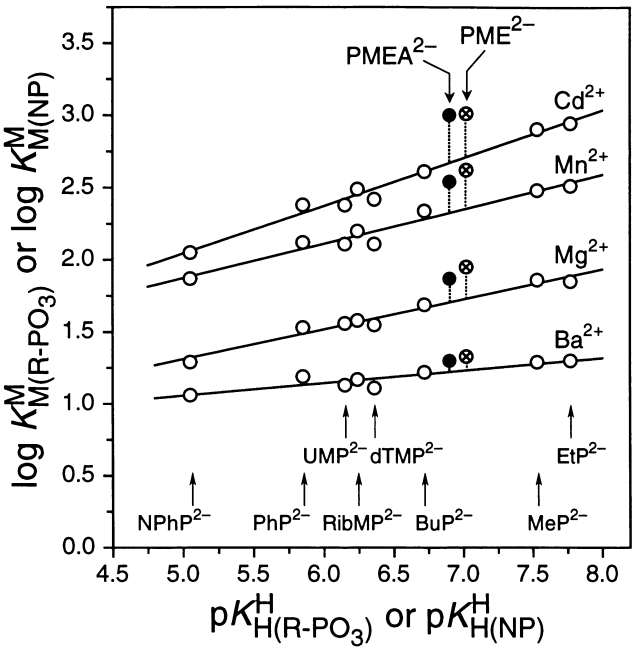

Fig. 4 Evidence for an enhanced stability of several M(PMEA) (●) and M(PME) (⊗) complexes, based on the relationship between log $K^{M}_{M(R\text{-}PO_3)}$ and $pK^{H}_{H(R\text{-}PO_3)}$ for the 1:1 complexes of Ba^{2+}, Mg^{2+}, Mn^{2+} and Cd^{2+} with some simple phosphate monoester or phosphonate ligands ($R\text{-}PO_3^{2-}$): 4-nitrophenyl phosphate ($NPhP^{2-}$), phenyl phosphate (PhP^{2-}), uridine 5′-monophosphate (UMP^{2-}), D-ribose 5-monophosphate ($RibMP^{2-}$), thymidine [= 1-(2′-deoxy-β-D-ribofuranosyl)thymine] 5′-monophosphate ($dTMP^{2-}$), *n*-butyl phosphate (BuP^{2-}), methanephosphonate (MeP^{2-}), and ethanephosphonate (EtP^{2-}) (from left to right) (○). The least-squares lines are drawn through the corresponding eight data sets [30]. The vertical broken lines emphasize the stability differences of the M(PMEA) (●) and M(PME) (⊗) complexes to the corresponding reference lines, which equal log $\Delta_{M/PMEA}$ and log $\Delta_{M/PME}$ (Eqn 6) (see also Table 3). The points due to the equilibrium constants for the PMEA (●) and PME (⊗) systems are taken from Tables 1, 2 and 8 of [30]. All plotted equilibrium constant values refer to aqueous solutions at 25 °C and $I = 0.1$ M ($NaNO_3$).

Table 4 Extent of chelate formation according to Equilibrium 1 for the M(PMEA) complexes as quantified by the dimensionless equilibrium constant K_I (Eqn 8) and the percentages of $M(PMEA)_{cl/O}$ (Eqn 9) (aqueous solution; 25 °C; $I = 0.1$ M, $NaNO_3$)*

M^{2+}	log $\Delta_{M/PMEA}$	$K_{I/O}$	% $M(PMEA)_{cl/O}$
Mg^{2+}	0.16 ± 0.05	0.45 ± 0.17	31 ± 8
Ca^{2+}	0.11 ± 0.07	0.29 ± 0.21	22 ± 13
Sr^{2+}	0.07 ± 0.05	0.17 ± 0.14	15 ± 10
Ba^{2+}	0.08 ± 0.06	0.20 ± 0.18	17 ± 12
Mn^{2+}	0.21 ± 0.08	0.62 ± 0.29	38 ± 11
Co^{2+}	0.28 ± 0.07†	0.91 ± 0.29	48 ± 8
Zn^{2+}	0.30 ± 0.10‡	1.00 ± 0.46	50 ± 12
Cd^{2+}	0.33 ± 0.06	1.14 ± 0.32	53 ± 7

* From table 10 of [30]. Regarding the error limits (3σ) see footnote * of Table 3.
† This value contains possibly a contribution from a nucleobase–Co^{2+} interaction (see Table 5).
‡ Estimate; see footnote † of Table 3.

$M(NP)_{cl/N7}$. This then gives rise to the two Equilibrium schemes 10 and 11:

$$M^{2+} + NP^{2-} \overset{K^{M}_{M(NP)_{op}}}{\rightleftharpoons} M(NP)_{op} \begin{matrix} \overset{K_{I/O}}{\rightleftharpoons} M(NP)_{cl/O} \\ \underset{K_{I/N7}}{\rightleftharpoons} M(NP)_{cl/N7} \end{matrix} \quad (10)$$

$$M^{2+} + NP^{2-} \overset{K^{M}_{M(NP)_{op}}}{\rightleftharpoons} M(NP)_{op} \overset{K_{I/O}}{\rightleftharpoons} M(NP)_{cl/O} \overset{K_{I/O/N3}}{\rightleftharpoons} M(NP)_{cl/O/N3} \quad (11)$$

For the M(PMEDAP) complexes it was shown that Scheme 10 operates [35], whereas for the M(PMEA) complexes it was concluded based on steric and chemical considerations [40,44], which were confirmed by NMR studies [43], that the dominating pathway involves N3 and thus, Scheme 11. Hence, next to $M(NP)_{op}$ and $M(NP)_{cl/O}$, the formation degree of $M(NP)_{cl/O/N3}$ needs to be determined. With this in mind the measured stability constant (Eqn 5) may be redefined [30,40] as given in Eqn 14 by considering scheme 11 and equations 12 and 13. The stability enhancement log Δ (Eqn 6) is connected with the overall intramolecular equilibrium constant $K_{I/tot}$ by Eqn 15 (for details see [30] and [40]). The corresponding results are summarized in Table 5. The now available data for M(PME-R) complexes [38] (see entries 1b–4b in Table 5, column 3) allowed a reevaluation of the M(PMEA) systems studied previously [30,40].

$$K^{M}_{M(NP)_{op}} = [M(NP)_{op}]/([M^{2+}][NP^{2-}]) \quad (12)$$

$$K_{I/O/N3} = [M(NP)_{cl/O/N3}]/[M(NP)_{cl/O}] \quad (13)$$

Table 5 Intramolecular equilibrium constants for the formation of the various M(PMEA) species as defined in Scheme 11, together with the percentages of the isomers (aqueous solution; 25 °C; $I = 0.1$ M, $NaNO_3$)*

No.*	System	log $\Delta_{M/PMEA}$ (Eqn 6)	$K_{I/tot}$ (Eqn 15)	% $M(PMEA)_{cl/tot}$ (analog. Eqn 9)	% $M(PMEA)_{op}$ (Eqns 11, 12)	
1a	Co(PMEA)	0.28 ± 0.07	0.91 ± 0.29	48 ± 8	52 ± 8	
2a	Ni(PMEA)	0.30 ± 0.07	1.00 ± 0.32	50 ± 8	50 ± 8	
3a	Cu(PMEA)	0.77 ± 0.07	4.89 ± 0.98	83 ± 3	17 ± 3	
4a	Cd(PMEA)	0.33 ± 0.06	1.14 ± 0.32	53 ± 7	47 ± 7	
No.*,†	**System**	**log $\Delta_{M/PME-R}$ (Eqn 6)**	**$K_{I/O}$ (Eqns 1, 8)**	**% $M(PMEA)_{cl/O}$ (Eqns 1, 11)**	**$K_{I/O/N3}$ (Eqns 13, 15c)**	**% $M(PMEA)_{cl/O/N3}$ (Eqn 11)**
1b	Co(PMEA)‡	0.20 ± 0.06	0.58 ± 0.22	30 ± 12	0.57 ± 0.78	18 ± 14‡
2b	Ni(PMEA)	0.14 ± 0.07	0.38 ± 0.22	19 ± 11	1.63 ± 1.74	31 ± 14
3b	Cu(PMEA)	0.48 ± 0.07	2.02 ± 0.49	34 ± 10	1.42 ± 0.76	49 ± 10
4b	Cd(PMEA)§	0.30 ± 0.05	1.00 ± 0.23	47 ± 13	0.14 ± 0.41	6 ± 15

* Entries 1a & 1b, 2a & 2b, etc. go together. Regarding the error limits (3σ) see footnote * of Table 3. The values in column 3 (1a–4a) are from Table 3, column 4 [30]. The values in column 6 regarding entries 1a-4a for the percentage of $M(PMEA)_{op}$ follow from 100 − % $M(PMEA)_{cl/tot}$.

† The values in column 3 for the M^{2+}/PME-R systems are from column 6 of Table 3 in [38] and they provide $K_{I/O}$; with the values now known for $K_{I/tot}$ and $K_{I/O}$ and Eqn 15c those for $K_{I/O/N3}$ may be calculated (column 6). The results for column 5 [% $M(PMEA)_{cl/O}$] were obtained with the left part of Eqn 8 using $K_{I/O}$ and percentage $M(PMEA)_{op}$. The values for percentage $M(PMEA)_{cl/O/N3}$ follow from the difference % $M(PMEA)_{cl/tot}$ − % $M(PMEA)_{cl/O}$; for further details see the footnotes in Table 4 or 11 in [40] or [30], respectively.

‡ The detection of the $Co(PMEA)_{cl/O/N3}$ isomer is at the limit of the method; however, its formation is probably real; application of a lower error limit, i.e. of 2σ gives: % $Co(PMEA)_{op} = 52 \pm 5$, % $Co(PMEA)_{cl/O} = 30 \pm 8$, and % $Co(PMEA)_{cl/O/N3} = 18 \pm 10$.

§ Cd(PMEA) was included only for reasons of comparison and to show that there is no evidence within the error limits for the formation of a $Cd(PMEA)_{cl/O/N3}$ species.

$$K^{M}_{M(NP)} = \frac{[M(NP)_{op}] + [M(NP)_{cl/O}] + [M(NP)_{cl/O/N3}]}{[M^{2+}][NP^{2-}]} \quad (14a)$$

$$= K^{M}_{M(NP)_{op}} + K_{I/O} \cdot K^{M}_{M(NP)_{op}} + K_{I/O} \cdot K_{I/O/N3} \cdot K^{M}_{M(NP)_{op}} \quad (14b)$$

$$= K^{M}_{M(NP)_{op}}(1 + K_{I/O} + K_{I/O} \cdot K_{I/O/N3}) \quad (14c)$$

$$K_{I/tot} = \frac{K^{M}_{M(NP)}}{K^{M}_{M(NP)_{op}}} - 1 = 10^{\log \Delta} - 1 \quad (15a)$$

$$= \frac{[M(NP)_{cl/tot}]}{[M(NP)_{op}]} = \frac{[M(NP)_{cl/O}] + [M(NP)_{cl/O/N3}]}{[M(NP)_{op}]} \quad (15b)$$

$$= K_{I/O} + K_{I/O} \cdot K_{I/O/N3} = K_{I/O}(1 + K_{I/O/N3}) \quad (15c)$$

To conclude, from Tables 4 and 5 it is clear that the five-membered chelate of Equilibrium 1 is of relevance and thus, metal ion coordination at the -PO_3^{2-} group of $PMEA^{2-}$ is further promoted by the interaction with the ether oxygen. This also holds for the P_α group of $PMEApp^{4-}$, in which the same steric unit occurs.

METAL ION-BINDING PROPERTIES OF $MePP^{3-}$

Methylphosphonylphosphate, CH_3-$P(O)_2^-$-O-PO_3^{2-}, can accept three protons giving $H_3(MePP)$. The first two protons are released outside of the physiological pH range with $pK_a < 2$ [45,46]. For the present only the equilibrium regarding the release of the final proton from the terminal β-phosphate group in $H(MePP)^{2-}$ (Eqn 16) and the formation of the $M(MePP)^-$ complexes (Eqn 17) are of relevance, though

$$H(MePP)^{2-} \rightleftharpoons H^+ + MePP^{3-} \quad (16a)$$

$$K^{H}_{H(MePP)} = [H^+][MePP^{3-}]/[H(MePP)^{2-}] \quad (16b)$$

$$M^{2+} + MePP^{3-} \rightleftharpoons M(MePP)^- \quad (17a)$$

$$K^{M}_{M(MePP)} = [M(MePP)^-]/([M^{2+}][MePP^{3-}]) \quad (17b)$$

the constants for the other protonated species were also estimated [46]. A simplified structure of a $M(MePP)^-$ complex is shown in Fig. 3 at the right and the corresponding stability constants are listed in column 2 of Table 6 [46]. The recently established correlations for M^{2+}-diphosphate monoester complex stabilities and diphosphate monoester β-group basicities [47], allow now an evaluation of the experimental data (Table 6), i.e. of the effect of the methylphosphonyl group on complex stability in comparison to that of the monoester phosphoryl group (see Fig. 3). A few straight-line plots [47] are shown in Fig. 5 in which the data points for the corresponding $M(MePP)^-$ complexes (•) [46] evidence that these are somewhat more stable than is expected on the basis of the basicity of the terminal β-phosphate group of $MePP^{3-}$ ($pK^{H}_{H(MePP)} = 6.57$ [46]).

Evaluation of this observation by using the straight-line equations (given in Table 4 of [47]) for the log $K^{M}_{M(R\text{-}DP)}$ vs. $pK^{H}_{H(R\text{-}DP)}$ plots, which allow with a known pK_a value of a monoprotonated diphosphate monoester the calculation of the stability of its corresponding $M(R\text{-}DP)^-$ complex, gives the results listed in column 3 of Table 6. The vertical distances seen in Fig. 5 (broken lines) correspond to the values given in the final column of Table 6, which follow from Eqn 18:

$$\log \Delta_{M/MePP} = \log K^{M}_{M(MePP)} - \log K^{M}_{M(MePP)_{calc.}} \quad (18)$$

The $M(MePP)^-$ complexes of the metal ions considered are on average by about 0.15 log unit more stable which is to be attributed [46] to the higher basicity of the phosphonyl group, compared to that of a phosphoryl unit as commonly present in a diphosphate monoester. For example, the release of the first proton from $H_2(MePP)^-$ occurs with $pK^{H}_{H_2(MePP)} = 1.85 \pm 0.03$ [46] compared to that from twofold protonated methyl diphosphate, $pK^{H}_{H_2(MeDP)} = 1.62 \pm 0.09$ [47], or uridine 5′-diphosphate, $pK^{H}_{H_2(UDP)} = 1.26 \pm 0.20$ [47]. Hence, for the phosphonyl group in $PMEApp^{4-}$ a higher metal ion affinity is expected than for the α-phosphate group of a nucleoside 5′-triphosphate.

Table 6 Stability constant comparisons for the $M(MePP)^-$ complexes between the measured (exptl [46]) (Eqn 17) and the calculated stability constants (calc.) based on the basicity of the terminal phosphate group of $MePP^{3-}$ ($pK^H_{H(MePP)} = 6.57 \pm 0.02$ [46]) and the baseline equations established previously [47], together with the resulting evidence for an increased complex stability, log $\Delta_{M/MePP}$, as defined by Eqn 18 (see also the plots in Fig. 5) (aqueous solution; 25 °C; $I = 0.1$ M, $NaNO_3$)*

	log $K^M_{M(MePP)}$		
M^{2+}	exptl	calc.	log $\Delta_{M/MePP}$†
Mg^{2+}	3.46 ± 0.03	3.38 ± 0.03	0.08 ± 0.04
Mn^{2+}	4.42 ± 0.02	4.26 ± 0.03	0.16 ± 0.04
Co^{2+}	3.98 ± 0.04	3.83 ± 0.05	0.15 ± 0.06
Ni^{2+}	3.78 ± 0.02	3.66 ± 0.06	0.12 ± 0.06
Cu^{2+}	5.66 ± 0.04	5.49 ± 0.04	0.17 ± 0.06
Zn^{2+}	4.46 ± 0.03	4.30 ± 0.03	0.16 ± 0.04
Cd^{2+}	4.60 ± 0.02	4.43 ± 0.03	0.17 ± 0.04

* From table 3 of [46]; in the same study [46] estimated values for the stability constants of the monoprotonated M(H;MePP) complexes are also listed; they all release their proton with $pK_a < 5.5$ [46]. Regarding the error limits (3σ) see footnote * of Table 3.

† For the Ca^{2+}, Sr^{2+}, and Ba^{2+} complexes of $MePP^{3-}$ the values for log $\Delta_{M/MePP}$ are 0.00 ± 0.04, −0.08 ± 0.05, and −0.14 ± 0.06, respectively [46]; these decreased complex stabilities are probably due to the formation of outersphere complexes; for details see [46].

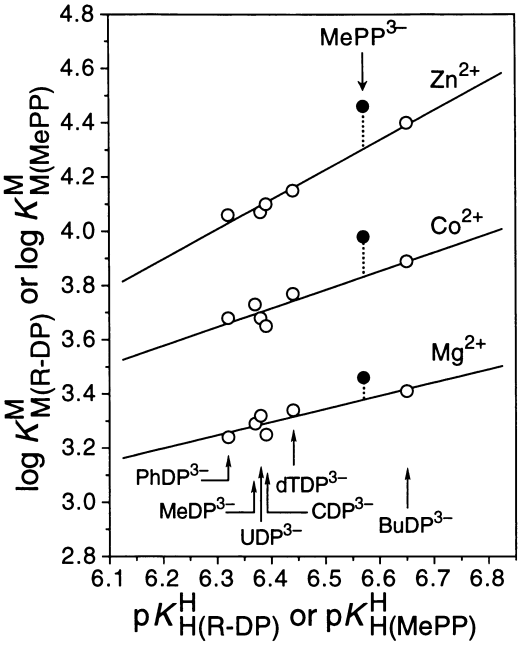

Fig. 5 Comparison of the $M(MePP)^-$ stabilities (●) with those of the M^{2+} complexes of diphosphate monoesters ($R\text{-}DP^{3-}$) (○) based on the relationship between log $K^M_{M(R\text{-}DP)}$ and $pK^H_{H(R\text{-}DP)}$ for the Mg^{2+}, Co^{2+}, and Zn^{2+} 1:1 complexes of phenyl diphosphate ($PhDP^{3-}$), methyl diphosphate ($MeDP^{3-}$), uridine 5′-diphosphate (UDP^{3-}), cytidine 5′-diphosphate (CDP^{3-}), thymidine (= 1-(2′-deoxy-β-D-ribofuranosyl)thymine) 5′-diphosphate ($dTDP^{3-}$) and *n*-butyl diphosphate ($BuDP^{3-}$). The least-squares lines are drawn through the indicated six (in the case of Zn^{2+} five) data sets; the corresponding straight-line equations are given in Table 4 of [47] (aqueous solution; 25 °C; $I = 0.1$ M, $NaNO_3$). The equilibrium constants for the M^{2+}/MePP systems are taken from Table 6.

CONCLUSIONS AND MECHANISTIC CONSIDERATIONS ON NUCLEIC ACID POLYMERASES

If a metal ion coordinates to a NTP^{4-} species forming a 1:1 complex, binding occurs at the β,γ-phosphate groups and depending on the metal ion also at the α group [48,49]. Upon formation of a 2:1 complex, the second metal ion coordinates to the α and β groups pushing thus the other one to the terminal (and most basic) γ group and this then gives rise to a dephosphorylation leading to NDP^{3-} and orthophosphate [22,23]. As indicated in the section on Metal Ions and Nucleic Acid Polymerases, this process is catalyzed, e.g. by kinases, leading to transphosphorylations.

In the case of nucleic acid polymerases the enzyme has to orientate the two metal ions such that a M(α)-M(β,γ) coordination of NTP^{4-} results (Fig. 2) which leads then to the release of diphosphate and the incorporation of the nucleotidyl unit into the growing nucleic acid chain. In the section on Metal Ions and Nucleic Acid Polymerases (Table 1) it was pointed out that $PMEApp^{4-}$ is initially a better substrate for DNA polymerases than $dATP^{4-}$. We are suggesting [21] that there are two reasons for this observation: metal ion binding to the α group is favored in $PMEApp^{4-}$ (i) due to the formation of the five-membered chelate with the ether oxygen (section on Evaluation of the Metal Ion-Binding Properties of PMEA), and (ii) due to the enhanced basicity of the α-phosphonyl group (section on Metal Ion-Binding Properties of $MePP^{3-}$). This situation then leads to a facilitated nucleophilic attack at P_α in M_2(PMEApp) compared to M_2(dATP); the corresponding structures [21] are shown in Fig. 6 [50]. The developed ideas concerning the importance of an enhanced metal ion binding to the α-phosph(on)ate group are in accord with indications in the literature, given unfortunately without experimental details [16], that PMEApp is a poorer substrate than ATP for ATPases because for these, like for kinases [25], a M(α,β)-M(γ) metal ion-coordination pattern is desirable [22,23]. Further support comes from the knowledge that the ether oxygen responsible for chelate formation (see Equilibrium 1) is compulsory for an antiviral activity; omitting, replacement by sulfur [51], or shifting the position of this oxygen leads to a reduction or even loss of the biological activity [6,19].

Of course, the nucleobase residue plays an important role in the anchoring process of the substrate and consequently, in the orientation of the metal ions in the active site cavity of the enzyme. It may interact with the protein either by stacking or hydrogen bonding with suitable amino acid side chains. As far as

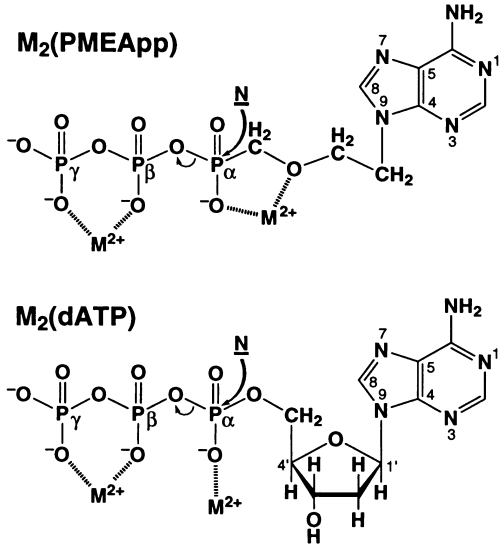

Fig. 6 Simplified structures of the M_2(PMEApp) and M_2(dATP) intermediates ready for the attack of a nucleophile (N) and on their way to the transition state in nucleic acid polymerases (see text) [21]. Both metal ions (usually Mg^{2+} [26,27,50]) are anchored [22,23] to amino acid side chains (often carboxylate groups of aspartate or glutamate units [26,27,50]) of the enzyme. The nucleophile N may in addition interact with M^{2+} at P_α and the adenine moiety may be replaced by any other nucleobase residue.

stacking is concerned, purines are favored over pyrimidines [52] and indeed, it appears from the data in Table 1 that the purines of the PME series (Fig. 1) are in general somewhat more effective than PMECpp; in fact, the other pyrimidines, PMEUpp and PMETpp, also inhibit polymerases only to the same or even a somewhat lesser extent than PMECpp [6,19].

The following observations also appear to be in accord with the view that the anchoring process is an important step: (i) PMEDAPpp is apparently a more effective inhibitor than PMEApp (Table 1) and it appears that its hydrogen bonding possibilities offer a larger variety for the anchoring process. (ii) There are also differences between the various polymerases; for example, DNA polymerase α is effectively inhibited by several of the pseudo-substrates (Table 1), whereas polymerase β is only little affected [19]; one is tempted to conclude that the pseudo-substrates fit well in the active site cavity of polymerase α but not of polymerase β and this might have to do with the missing sugar part or a different local intrinsic dielectric constant which can affect complex stability considerably [53]. (iii) Similarly, since PMEC is devoid of a significant biological activity [6], whereas HPMPC (see Fig. 7), also known as cidofovir [5], is used in the treatment of cytomegalovirus-induced retinitis [54] and other virus-induced diseases [55], one is tempted to suggest that the hydroxy methyl residue facilitates initially the anchoring process by hydrogen bonding with the OH group (aside from the fact that incorporation of HPMPC due to the OH group does not immediately lead to a termination of the growing nucleic acid chain [5]). (iv) That the activity spectrum of PMEA (Fig. 1) and HPMPA (Fig. 7) only partially overlaps [4,6] may also originate from variations of the anchoring process; stacking will be alike, but the OH group of HPMPA allows in addition hydrogen bonding and its incorporation into the growing nucleic acid chain does not lead to the immediate termination of the latter [18], since the OH group is kind of an equivalent of the 3′-OH group present in the natural substrates. Hence, further selectivities in the activity spectrum of these compounds may be achieved by variations of the nucleobase moieties and possibly sophisticated mimics of the (2′-deoxy)-ribose residues.

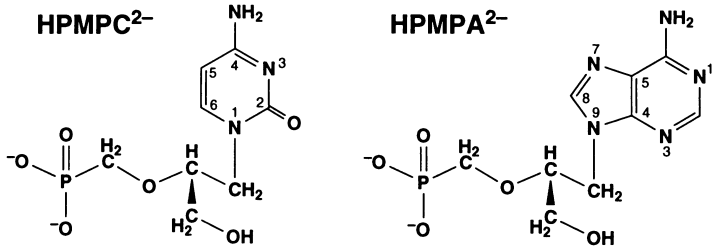

Fig. 7 Chemical structures of the dianions of (*S*)-1-[3-hydroxy-2-(phosphonomethoxy)propyl]cytosine ($HPMPC^{2-}$) and (*S*)-9-[3-hydroxy-2-(phosphonomethoxy)propyl]adenine ($HPMPA^{2-}$).

In conclusion, however, most important is the above described insight that favored metal ion-binding properties of the P_α group are important for obtaining a high biological activity of the nucleotide analogue; this result should be kept in mind in the search for new antivirally active analogues.

ABBREVIATIONS

See the title and also Figures 1, 3–5, and 7. ANP^{2-}, acyclic-nucleoside monophosphonate (like $PMEA^{2-}$); $ANPpp^{4-}$, diphosphorylated ANP^{2-} (like $PMEApp^{4-}$ or $PMEDAPpp^{4-}$); $dCTP^{4-}$, 2′-deoxycytidine 5′-triphosphate; $dGTP^{4-}$, 2′-deoxyguanosine 5′-triphosphate; $dNMP^{2-}$ or $dNTP^{4-}$, 2′-deoxynucleoside 5′-mono- or triphosphate (like $dAMP^{2-}$, $dCMP^{2-}$ or $dATP^{4-}$, $dCTP^{4-}$); M^{2+}, divalent metal ion; NMP^{2-}, NDP^{3-} or NTP^{4-}, nucleoside 5′-mono-, di- or triphosphate; NP^{2-}, nucleobase phosph(on)ate derivative; $PMEGpp^{4-}$, $PMETpp^{4-}$ or $PMEUpp^{4-}$, diphosphorylated 9-[2-(phosphonomethoxy)ethyl]guanine (PMEG), 1-[2-(phosphonomethoxy)ethyl]thymine (PMET) or 1-[2-(phosphonomethoxy)ethyl]uracil (PMEU). Species given in the text without a charge either do not carry one or represent the species in general (i.e., independent from their protonation degree); which of the two versions applies is always clear from the context.

ACKNOWLEDGEMENT

The competent technical assistance in the preparation of the manuscript and the figures of *Mrs. Rita Baumbusch* and *Dr Larisa E. Kapinos*, respectively, as well as the support of the research of my group on antiviral nucleotide analogues by the *Swiss National Science Foundation* and the *Swiss Federal Office for Education & Science* within the COST D8 programme is gratefully acknowledged.

REFERENCES

1 E. De Clercq. *Collect. Czech. Chem. Commun.* **63,** 449–479 (1998).

2 H. Sigel, A. Sigel, eds. Interrelations among metal ions, enzymes, and gene expression. In *Metal Ions in Biological Systems,* Vol. 25, pp. 1–557. Marcel Dekker Inc., New York/Basel (1989).

3 A. Sigel, H. Sigel, eds. Interactions of metal ions with nucleotides, nucleic acids, and their constituents. In *Metal Ions in Biological Systems*, Vol. 32, pp. 1–814. Marcel Dekker Inc., New York/Basel (1996).

4 A. Holý. In *Advances in Antiviral Drug Design* (E. De. Clercq, ed.), Vol. 1, pp. 179–231. JAI Press Inc, Greenwich, CT (1993).

5 E. De Clercq. *Collect. Czech. Chem. Commun.* **63,** 480–506 (1998).

6 A. Holý, E. De Clercq, I. Votruba. *ACS Symp Ser.* **401,** 51–71 (1989).

7 E. De Clercq. *Pure Appl. Chem.* **70,** 567–577 (1998).

8 C. A. Blindauer, A. Holý, H. Dvořáková, H. Sigel. *J. Chem. Soc., Perkin Trans.* **2,** 2353–2363 (1997).

9 H. Sigel, C. A. Blindauer, A. Holý, H. Dvořáková. *Chem. Commun.* 1219–1220 (1998).

10 H. Sigel. *Pure Appl. Chem.* **70,** 969–976 (1998).

11 R. B. Martin, Y. H. Mariam. *Met. Ions Biol. Syst.* **8,** 57–124 (1979).

12 R. Tribolet, H. Sigel. *Eur. J. Biochem.* **163,** 353–363 (1987).

13 K. Aoki. *Met. Ions Biol. Syst.* **32,** 91–134 (1996); this is Chapter 4 in ref. [3].

14 D. B. Davies, P. Rajani, H. Sadikot. *J. Chem. Soc., Perkin Trans.* **2**, 279–285 (1985).

15 F. Franek, A. Holý, I. Votruba, T. Eckschlager. *Internat. J. Oncology* **14,** 745–752 (1999).

16 J. Balzarini, Z. Hao, P. Herdewijn, D. G. Johns, E. De Clercq. *Proc. Natl. Acad. Sci. USA* **88,** 1499–1503 (1991).

17 A. Merta, I. Votruba, I. Rosenberg, M. Otmar, H. Hřebabecký, R. Bernaerts, A. Holý. *Antiviral Res.* **13,** 209–218 (1990).

18 P. Kramata, I. Votruba, B. Otová, A. Holý. *Mol Pharmacol.* **49,** 1005–1011 (1996).

19 A. Holý, I. Votruba, A. Merta, J. Černý, J. Veselý, J. Vlach, K. Šedivá, I. Rosenberg, M. Otmar, H. Hřebabecký, M. Trávníček, V. Vonka, R. Snoeck, E. De Clercq. *Antiviral Res.* **13,** 295–311 (1990).

20 A. S. Mildvan. *Magnesium* **6,** 28–33 (1987).

21 H. Sigel, B. Song, C. A. Blindauer, L. E. Kapinos, F. Gregáň, N. Prónayová. *Chem. Commun.* 743–744 (1999).

22 H. Sigel, F. Hofstetter, R. B. Martin, R. M. Milburn, V. Scheller-Krattiger, K. H. Scheller. *J. Am. Chem. Soc.* **106**, 7935–7946 (1984).

23 H. Sigel. *Coord. Chem. Rev.* **100,** 453–539 (1990).

24 H. Sigel. *Inorg. Chim. Acta* **198–200,** 1–11 (1992).

25 L. W. Tari, A. Matte, H. Goldie, L. T. J. Delbaere. *Nature Struct. Biol.* **4,** 990–994 (1997).

26 (a) H. Pelletier, M. R. Sawaya, A. Kumar, S. H. Wilson, J. Kraut. *Science* **264**, 1891–1903 (1994). (b) H. Pelletier. *Science* **266**, 2025–2026 (1994). (c) H. Pelletier, M. R. Sawaya, W. Wolfle, S. H. Wilson, J. Kraut. *Biochemistry* **35**, 12762–12777 (1996).

27 (a) T. A. Steitz. *Nature* **391**, 231–232 (1998). (b) C. A. Brautigam, T. A. Steitz. *Curr. Opinion Struct Biol.* **8**, 54–63 (1998).

28 H. Sigel, C. P. Da Costa, B. Song, P. Carloni, F. Gregáň. *J. Am. Chem. Soc.* **121,** 6248–6257 (1999).

29 A. Saha, N. Saha, L.-n. Ji, J. Zhao, F. Gregáň, S. A. A. Sajadi, B. Song, H. Sigel. *JIBC* **1,** 231–238 (1996).

30 H. Sigel, D. Chen, N. A. Corfù, F. Gregáň, A. Holý, M. Strašák. *Helv. Chim. Acta* **75,** 2634–2656 (1992).

31 S. S. Massoud, H. Sigel. *Inorg. Chem.* **27,** 1447–1453 (1988).

32 H. Sigel, S. S. Massoud, R. Tribolet. *J. Am. Chem. Soc.* **110,** 6857–6865 (1988).

33 H. Sigel, S. S. Massoud, N. A. Corfù. *J. Am. Chem. Soc.* **116,** 2958–2971 (1994).

34 L. E. Kapinos, G. Kampf, R. Griesser, B. Lippert, H. Sigel. *Chimia* **53,** in press (2000).

35 C. A. Blindauer, T. I. Sjåstad, A. Holý, E. Sletten, H. Sigel. *J. Chem. Soc., Dalton Trans.* 3661–3671 (1999).

36 Y. Kinjo, L.-n. Ji, N. A. Corfù, H. Sigel. *Inorg. Chem.* **31,** 5588–5596 (1992).

37 B. Song, G. Feldmann, M. Bastian, B. Lippert, H. Sigel. *Inorg. Chim. Acta* **235,** 99–109 (1995).

38 C. A. Blindauer, A. Holý, H. Sigel. *Collect. Czech. Chem. Commun.* **64,** 613–632 (1999).

39 H. Sigel, A. D. Zuberbühler, O. Yamauchi. *Anal. Chim. Acta* **255,** 63–72 (1991).

40 H. Sigel. *Coord. Chem. Rev.* **144,** 287–319 (1995).

41 H. Sigel, B. Song. *Met. Ions Biol. Syst.* **32,** 135–205 (1996); this is Chapter 5 in ref. [3].

42 R. B. Martin, H. Sigel. *Comments Inorg. Chem.* **6,** 285–314 (1988).

43 C. A. Blindauer, A. H. Emwas, A. Holý, H. Dvořáková, E. Sletten, H. Sigel. *Chem. Eur. J.* **3,** 1526–1536 (1997).

44 H. Sigel. *J. Indian Chem. Soc.* **74,** 261–271 (1997) [P. Ray Award Lecture].

45 B. Song, S. A. A. Sajadi, F. Gregáň, N. Pronáyová, H. Sigel. *Inorg. Chim. Acta* **273,** 101–105 (1998).

46 B. Song, J. Zhao, F. Gregáň, N. Pronáyová, S. A. A. Sajadi, H. Sigel. *Metal-Based Drugs* **6,** 321–328 (1999).

47 S. A. A. Sajadi, B. Song, F. Gregáň, H. Sigel. *Inorg. Chem.* **38,** 439–448 (1999).

48 H. Sigel. *Chem. Soc. Reviews* **22,** 255–267 (1993).

49 H. Sigel. *Eur. J. Biochem.* **165,** 65–72 (1987).

50 C. Klevickis, C. M. Grisham. *Met. Ions Biol. Syst.* **32,** 1–26 (1996); this is Chapter 1 in ref. [3].

51 D. Villemin, F. Thibault-Starzyk. *Synthet. Commun.* **23,** 1053–1059 (1993).

52 O. Yamauchi, A. Odani, H. Masuda, H. Sigel. *Met. Ions Biol. Syst.* **32,** 207–270 (1996); this is Chapter 6 in ref. [3].

53 (a) D. Chen, F. Gregáň, A. Holý, H. Sigel. *Inorg. Chem.* **32**, 5377–5384 (1993). (b) D. Chen, M. Bastian, F. Gregáň, A. Holý, H. Sigel. *J. Chem. Soc., Dalton Trans.* 1537–1546 (1993).

54 J. P. Lalezari, G. N. Holland, F. Kramer, G. F. McKinley, C. A. Kemper, D. V. Ives, R. Nelson, W. D. Hardy, B. D. Kuppermann, D. W. Northfelt, M. Youle, M. Johnson, R. A. Lewis, D. V. Weinberg, G. L. Simon, R. A. Wolitz, A. E. Ruby, R. J. Stagg, H. S. Jaffe. *J. Acquir. Immune Defic. Syndr. Hum. Retrovirol.* **17,** 339–344 (1998).

55 R. Snoeck, W. Wellens, C. Desloovere, M. Van Ranst, L. Naesens, E. De Clercq, L. Feenstra. *J. Med. Virol.* **54,** 219–225 (1998); G. Blick, M. Whiteside, P. Griegor, U. Hopkins, T. Garton, L. LaGravinese. *Clin. Infect. Dis.* **26,** 191–192 (1998); A. E. LoPresti, J. F. Levine, G. B. Munk, C. Y. Tai, D. B. Mendel. *Clin. Infect. Dis.* **26,** 512–513 (1998).